

## Supplementary Information

### Catalytic covalent organic frameworks via pore surface engineering

Hong Xu,<sup>a</sup> Xiong Chen,<sup>a</sup> Jia Gao,<sup>a</sup> Jianbin Lin,<sup>a</sup> Matthew Addicoat,<sup>b</sup>  
Stephan Irle,<sup>b</sup> and Donglin Jiang\*<sup>a</sup>

<sup>a</sup>*Department of Materials Molecular Science, Institute for Molecular Science, National Institutes of Natural Sciences, 5-1 Higashiyama, Myodaiji, Okazaki 444-8787, Japan*

<sup>b</sup>*WPI-Research Initiative-Institute of Transformative Bio-Molecules and Department of Chemistry, Graduate School of Science, Nagoya University, Furo-cho, Chikusa-ku, Nagoya 464-8602, Japan*

*Corresponding author: Professor Donglin Jiang (e-mail: jiang@ims.ac.jp)*

#### Table of Contents

A. Methods .....	2
B. Materials and synthetic procedures.....	4
C. Reaction conditions.....	6
D. Elemental analysis results.....	7
E. Structural simulation .....	8
F. FT-IR spectra.....	9
G. Nitrogen sorption isotherm curves, pore size and pore size distribution profiles .....	10
H. Michael addition reactions.....	13
I. Recycling results .....	17
J. Supporting references .....	18

## A. Methods

Thin-layer chromatography (TLC) plates were visualized by exposure to ultraviolet light and/or developed with iodine vapor. Flash column chromatography was carried out with silica gel (200-300 mesh).  $^1\text{H}$  nuclear magnetic resonance (NMR) spectra were recorded on JEOL models JNM-LA400 NMR spectrometers, where chemical shifts ( $\delta$  in ppm) were determined with a residual proton of the solvent as standard. Fourier transform infrared (IR) spectra were recorded on a JASCO model FT-IR-6100 infrared spectrometer. Matrix-assisted laser desorption ionization time-of-flight mass (MALDI-TOF MS) spectra were recorded on an Applied Biosystems BioSpectrometry model Voyager-DE-STR spectrometer in reflector or linear mode. X-ray diffraction (XRD) data were recorded on a Rigaku model RINT Ultima III diffractometer by depositing powder on glass substrate, from  $2\theta = 1.5^\circ$  up to  $60^\circ$  with  $0.02^\circ$  increment. Nitrogen sorption isotherms were measured at 77 K with a Micromeritics Instrument Corporation model 3Flex surface characterization analyzer. The Brunauer-Emmett-Teller (BET) method was utilized to calculate the specific surface areas. By using the non-local density functional theory (NLDFFT) model, the pore volume was derived from the sorption curve. Elemental analysis was performed on a Yanako model CHN CORDER MT-6 elemental analyzer. High performance liquid chromatography were performed on a JASCO model HPLC model with Daicel chiral AD-H and OD-H columns with *i*-PrOH/*n*-hexane as the eluent.

The molecular structure and electronic properties of monolayer and stacked  $\text{H}_2\text{P-COF}$  isomers were determined using the density-functional tight-binding (DFTB) method including Lennard-Jones (LJ) dispersion. The corresponding LJ and crystal stacking energies as well as the HOMO-LUMO energy gaps were computed. The calculations were carried out with the DFTB+ program package version 1.2.<sup>S1</sup> DFTB is an approximate density functional theory method based on the tight binding approach and utilizes an optimized minimal LCAO Slater-type all-valence basis set in combination with a two-center approximation for Hamiltonian matrix elements. The Coulombic interaction between partial atomic charges was determined using the self-consistent charge (SCC) formalism. Lennard-Jones type dispersion was employed in all calculations to describe van der Waals (vdW) and p-stacking interactions. The lattice dimensions were optimized simultaneously with the geometry. Standard DFTB parameters for X–Y element pair

(X, Y = C, O, H and N) interactions were employed from the mio-0-1 set.<sup>S2</sup> The optimal single layer 2D model system consisted of 110 atoms for the monomer. The monomer had an optimal lattice parameter of  $a = b = 25.5 \text{ \AA}$ . Using the optimized monomer, three different stacking configurations: perfect AA, AA slip-stacked by  $0.8 \text{ \AA}$  in the  $a$  and  $b$  directions, and AB were optimized. The third dimension of the lattice,  $c$  was initialized at  $3.5 \text{ \AA}$  for all structures.

Orientation of catalyst groups is beginning with the optimized H<sub>2</sub>P-COF, the hydroxyl-hydrogen atoms of the central phenyl group were replaced with the triazole-pyrrolidine group. The triazole-pyrrolidine group is conformationally flexible, and so in order to determine its orientation within the COF, a Genetic Algorithm (GA) previously optimized for the determination of molecular conformers was employed.<sup>S3</sup> The optimum structures and corresponding electronic properties of stacked isomers of [Pyr]<sub>50</sub>-H<sub>2</sub>P-COF were calculated using density-functional tight-binding (DFTB) method including Lennard-Jones (LJ) dispersion. For the monolayer structures, the optimized lattice constant is,  $a = b = 25.5 \text{ \AA}$ . To avoid H-H overlap with the porphyrin ring, the adjacent phenyl groups rotate to an almost perpendicular orientation, with a dihedral angle of  $74^\circ$  and the central ring tilts in the opposing direction by  $38^\circ$ . Using the optimal monolayer structure, three stacked configurations; AA, slipped-AA, and AB were generated and optimized. The interlayer stacking distances, and the corresponding LJ and crystal stacking energies per monolayer of each structure are shown in Table S3.

## B. Materials and synthetic procedures

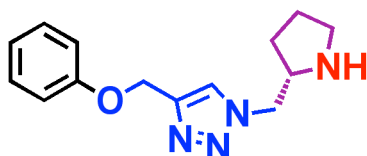
Dehydrated *N,N*-dimethylformide (DMF), *N,N*-dimethylacetamide (DMAc), dehydrated tetrahydrofuran (THF), and *o*-dichlorobenzene (*o*-DCB) were purchased from Kanto Chemicals. Pyrrole, *p*-nitrobenzaldehyde, hydrobromic acid, *p*-toluenesulfonyl chloride, trifluoroacetic acid, toluene, dioxane, mesitylene, 1-butanol, ethanol, and acetic acid were purchased from Wako Chemicals. Propionic acid, propargyl bromide, 1,4-dimethoxybenzene, *N*-(*tert*-butoxycarbonyl)-L-prolinol, *tert*-butyl alcohol, propionaldehyde, valeraldehyde and benzoic acid were purchased from TCI. *trans-beta*-Nitrostyrene, *N,N*-diisopropylethylamine, *trans*-4-chloro-*beta*-nitrostyrene, *trans*-4-bromo-*beta*-nitrostyrene, *trans*-4-fluoro-*beta*-nitrostyrene, *trans*-2-chloro-*beta*-nitrostyrene, and *trans*-4-methoxy-*beta*-nitrostyrene were purchased from Sigma-Aldrich Co.

5,10,15,20-Tetrakis(4'-tetraphenylamino)porphyrin (H<sub>2</sub>P) was prepared using a literature procedure.<sup>S4</sup> 2,5-Dihydroxyterephthalaldehyde (DHTA) and 2,5-bis(2-propynyloxy) terephthalaldehyde (BPTA) were synthesized according to the reported methods.<sup>S5, S6</sup> (*S*)-2-(Azidomethyl)pyrrolidine was synthesized using a reported method.<sup>S7</sup>

**[HC≡C]<sub>x</sub>-H<sub>2</sub>P-COFs.** An *o*-DCB/BuOH (0.5 mL / 0.5 mL) mixture of H<sub>2</sub>P (0.022 mmol, 14.9 mg) and DHTA/BPTA (total 0.044 mmol) at different molar ratios of 100/0, 75/25, 50/50, 25/75, and 0/100 in the presence of acetic acid catalyst (3 M, 0.1 mL) in a Pyrex tube (10 mL) was degassed by three freeze–pump–thaw cycles. The tube was sealed off by flame and heated at 120 °C for 3 days. The precipitate was collected via centrifuge, washed with THF for 6 times, and washed with acetone 3 times. The powder was dried at 120 °C under vacuum overnight to give the corresponding COFs in isolated yields of 80%, 72%, 69%, 86%, and 80% for the H<sub>2</sub>P-COF, [HC≡C]<sub>25</sub>-H<sub>2</sub>P-COF, [HC≡C]<sub>50</sub>-H<sub>2</sub>P-COF, [HC≡C]<sub>75</sub>-H<sub>2</sub>P-COF, and [HC≡C]<sub>100</sub>-H<sub>2</sub>P-COF, respectively.

The amorphous nonporous polymers 1 and 2 were synthesized in DMAc, according to this method under otherwise same conditions. (Table S1, ESI†) The ethynyl contents in the COFs as estimated by considering the elemental analysis results together with particle size and remained edges units were close to the theoretical results.

**[Pyr]<sub>X</sub>-H<sub>2</sub>P-COFs.** A toluene/*tert*-butanol (0.8 mL / 0.2 mL) mixture of [HC≡C]<sub>25</sub>-H<sub>2</sub>P-COF (20 mg) in the presence of CuI (2 mg) and DIPEA (40 μL) in a Pyrex tube (10 mL) was added with (*S*)-2-(azidomethyl)pyrrolidine (toluene solution; 1 M; 21 μL). The tube was degassed via three freeze–pump–thaw cycles and the mixture was stirred at room temperature for 24 h. The precipitate was collected via centrifuge, washed with ethanol 5 times, and dried at room temperature under vacuum, to produce [Pyr]<sub>25</sub>-H<sub>2</sub>P-COF as a deep brown solid in quantitative yield. The ethynyl groups were quantitatively reacted with the azide units as evident by the IR spectra. The click reaction of [HC≡C]<sub>X</sub>-H<sub>2</sub>P-COFs (X = 50, 75, and 100) with (*S*)-2-(azidomethyl)pyrrolidine were performed according to this method under otherwise same conditions.



**Control: (*S*)-4-(Phenoxymethyl)-1-(pyrrolidin-2-ylmethyl)-1H-1,2,3-triazole**

**(*S*)-4-(Phenoxymethyl)-1-(pyrrolidin-2-ylmethyl)-1H-1,2,3-triazole.** The click reaction to synthesize this monomeric catalyst control was prepared according to the above procedure for [Pyr]<sub>X</sub>-H<sub>2</sub>P-COF, using phenyl propargyl ether (toluene solution; 1M, 80 μL) in place of [HC≡C]<sub>X</sub>-H<sub>2</sub>P-COFs as a reactant.

**Michael addition reaction.** To an EtOH/H<sub>2</sub>O (1/1 v/v 0.5 mL) suspension of [Pyr]<sub>25</sub>-H<sub>2</sub>P-COF was added with aldehyde (1.0 mmol), nitrostyrene (0.1 mmol), and benzoic acid (0.1 mmol). The mixture was stirred at room temperature for a period to reach 100% conversion. After addition of EtOH, the organic layer was removed via centrifuge. The catalyst was washed with EtOH twice and with ethyl acetate 3 times, the organic layer was then combined and concentrated under reduced pressure. <sup>1</sup>H-NMR spectra were utilized to calculate diastereomeric ratio (dr). The enantiomeric excess (ee) was determined by HPLC on a chiral phase chiralpak AD-H or OD-H column.

**Recycle use of [Pyr]<sub>25</sub>-H<sub>2</sub>P-COF.** The COF catalyst was recovered via centrifuge, washed with ethyl acetate and a mixture of triethylamine/ethanol solution (5% v) to remove the product and reactants and simply dried before reuse.

## C. Reaction conditions

**Table S1.** Reaction conditions of preparing [HC≡C]<sub>x</sub>-H<sub>2</sub>P-COFs.

X	Solvent	Catalyst: Acetic Acid	Temp. (°C)	Time (day)	Yield (%)	XRD Intensity (Counts)
50	Mesitylene/Dioxane 0.5 mL/0.5 mL	(6M), 0.1 mL	120	3	60	10010
	Mesitylene/Dioxane 0.5 mL/0.5 mL	(6M), 0.1 mL	120	5	69	3073
	Mesitylene/Dioxane 0.5 mL/0.5 mL	(6M), 0.1 mL	120	15	76	1787
	Mesitylene/Dioxane 0.25 mL/0.75 mL	(6M), 0.1 mL	120	3	60	5705
	Mesitylene/Dioxane 1.0 mL/1.0 mL	(6M), 0.2 mL	120	3	10	No Peak
	<i>o</i> -DCB/BuOH 0.5 mL/0.5 mL	(3M), 0.1 mL	120	3	69	7536
	<i>o</i> -DCB/BuOH 0.5 mL/0.5 mL	(6M), 0.1 mL	120	3	75	4003
	<i>o</i> -DCB/BuOH 0.5 mL/0.5 mL	(6M), 0.1 mL	120	5	80	2305
	<i>o</i> -DCB/BuOH 0.5 mL/0.5 mL	-	120	5	66	1150
	<i>o</i> -DCB/BuOH 0.9 mL/0.1 mL	(6M), 0.1 mL	120	5	82	3231
	DMAc 1mL	-	120	3	79 <sup>a</sup>	No Peak
	<i>m</i> -cresol 1mL	-	120	5		No Peak
	<i>m</i> -cresol 1mL	(6M), 0.1 mL	120	5		No Peak
	<i>o</i> -DCB 1mL	(6M), 0.1 mL	120	5		No Peak
	Dioxane 1mL	(6M), 0.1 mL	120	5		No Peak
0	<i>o</i> -DCB/BuOH 0.5 mL/0.5 mL	(3M), 0.1 mL	120	3	80	14666
25	<i>o</i> -DCB/BuOH 0.5 mL/0.5 mL	(3M), 0.1 mL	120	3	72	14095
	<i>o</i> -DCB/BuOH 0.5 mL/0.5 mL	(6M), 0.1 mL	120	5	82	6695
	DMAc 1 mL	(3M), 0.1 mL	120	3	73	4096
	DMAc 1 mL	-	120	1	82 <sup>b</sup>	No Peak
75	<i>o</i> -DCB/BuOH 0.5 mL/0.5 mL	(3M), 0.1 mL	120	3	86	2343
100	<i>o</i> -DCB/BuOH 0.5 mL/0.5 mL	(3M), 0.1 mL	120	3	80	1052

<sup>a</sup> Amorphous and Nonporous Polymer 2

<sup>b</sup> Amorphous and Nonporous Polymer 1

## D. Elemental analysis results

**Table S2.** Elemental analysis of the COFs.

COFs		C (%)	H (%)	N (%)
H <sub>2</sub> P-COF	Calcd.	77.07	4.1	11.98
	Found	73.9	5.23	9.57
[HC≡C] <sub>25</sub> -H <sub>2</sub> P-COF	Calcd.	77.76	4.14	11.52
	Found	75.12	5.76	8.81
[HC≡C] <sub>50</sub> -H <sub>2</sub> P-COF	Calcd.	78.4	4.19	11.08
	Found	75.45	5.29	9.24
[HC≡C] <sub>75</sub> -H <sub>2</sub> P-COF	Calcd.	78.99	4.22	10.68
	Found	74.27	4.8	8.94
[HC≡C] <sub>100</sub> -H <sub>2</sub> P-COF	Calcd.	79.54	4.26	10.31
	Found	75.29	4.83	8.62
[Pyr] <sub>25</sub> -H <sub>2</sub> P-COFs	Calcd.	74.3	4.58	15.29
	Found	71.99	4.69	12.51
[Pyr] <sub>50</sub> -H <sub>2</sub> P-COFs	Calcd.	72.25	4.95	17.74
	Found	66.53	5.09	13.5
[Pyr] <sub>75</sub> -H <sub>2</sub> P-COFs	Calcd.	70.67	5.22	19.62
	Found	63.89	4.86	15.06
[Pyr] <sub>100</sub> -H <sub>2</sub> P-COFs	Calcd.	69.42	5.45	21.12
	Found	65.46	5.15	16.82
Amorphous and Nonporous Polymer 1	Calcd.	74.3	4.58	15.29
	Found	67.41	4.65	11.57
Amorphous and Nonporous Polymer 2	Calcd.	72.25	4.95	17.74
	Found	67.19	5.25	13.39

## E. Structural simulation

**Table S3.** The total DFTB energies, Lennard-Jones contributions (LJ), and the crystal stacking energies per unit cell for the H<sub>2</sub>P-COF and [Pyr]<sub>25</sub>-H<sub>2</sub>P-COF.

Stacking Mode	<i>c</i> (Å)	Total DFTB Energy (a.u.)	LJ energy (a.u.)	Total crystal stacking energy (kcal mol <sup>-1</sup> )
Monolayer		-149.2124992	0.5816	
AA H <sub>2</sub> P-COF	3.96	-298.6138679	0.9674	59.26
Slipped AA H <sub>2</sub> P-COF (0.8 Å)	3.63	-298.6262435	0.9603	63.14
AB H <sub>2</sub> P-COF	3.22	-298.550363	1.0437	39.33
Slipped AA [Pyr] <sub>25</sub> -H <sub>2</sub> P-COF	4.09	-409.182501	1.2833	92.83

## F. FT-IR spectra

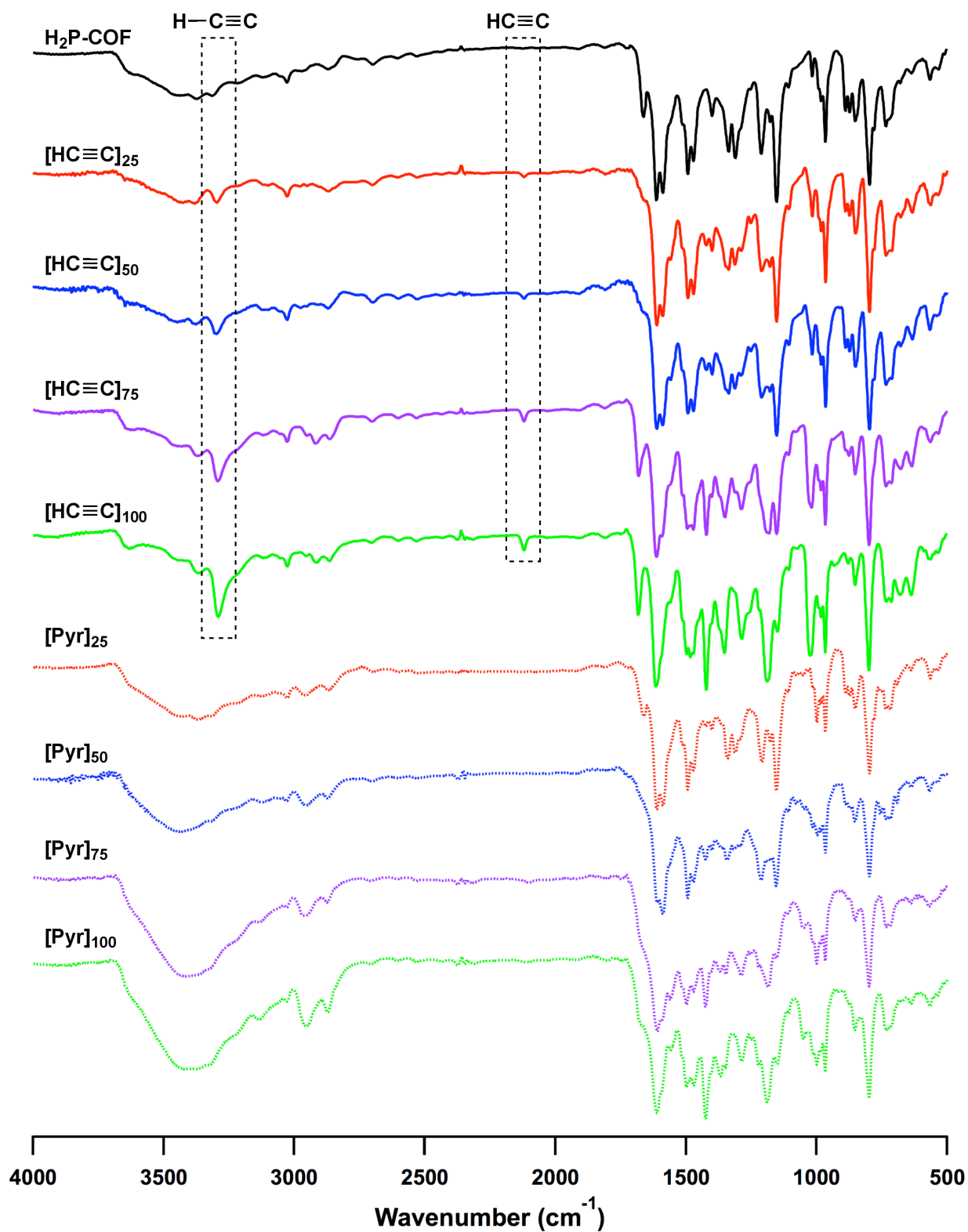
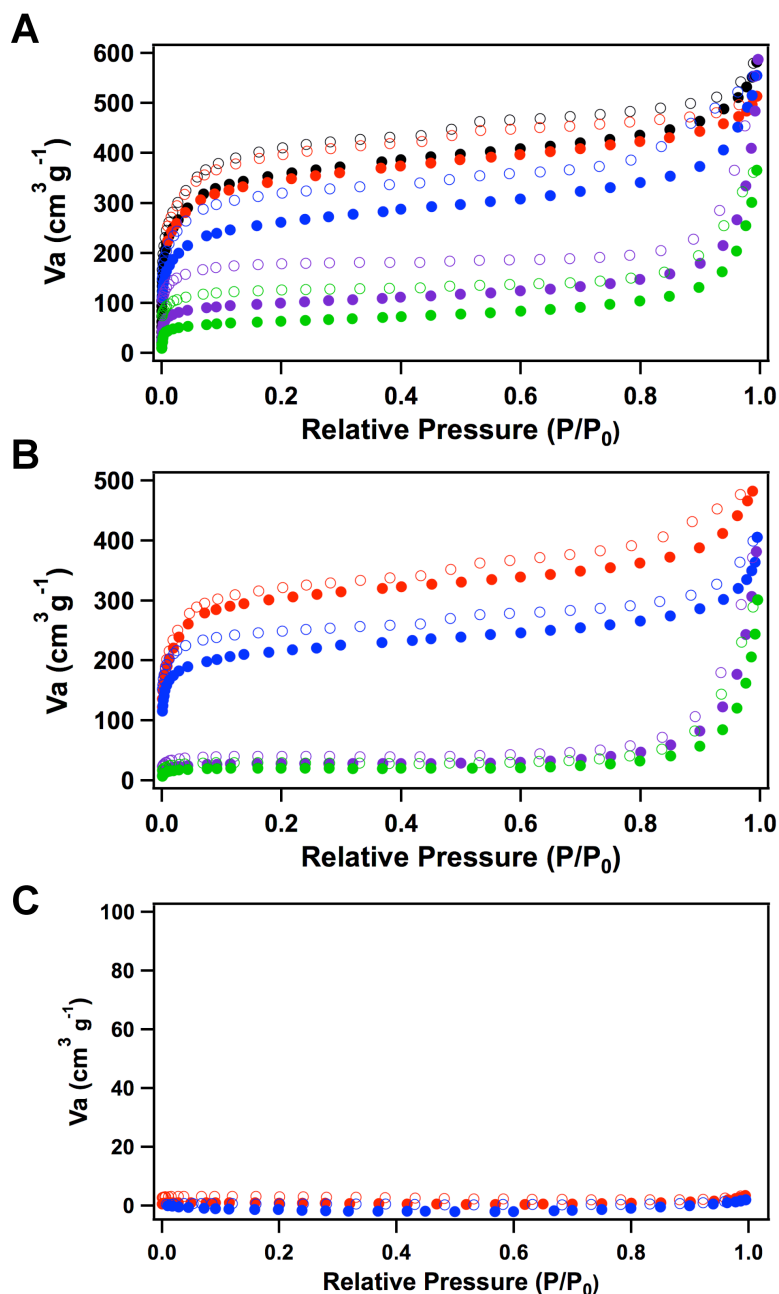


Fig. S1 IR Spectra of  $\text{H}_2\text{P-COF}$ ,  $[\text{HC}\equiv\text{C}]_x\text{-H}_2\text{P-COFs}$ , and  $[\text{Pyr}]_x\text{-H}_2\text{P-COFs}$ .

## G. Nitrogen sorption isotherm curves, pore size and pore size distribution profiles



**Fig. S2** Nitrogen sorption isotherm profiles of (A)  $\text{H}_2\text{P-COF}$  (black) and  $[\text{HC}\equiv\text{C}]_X\text{-H}_2\text{P-COFs}$  (X=25: red, X = 50: blue, X = 75: purple, X = 100: green), (B)  $[\text{Pyr}]_X\text{-H}_2\text{P-COFs}$  (X=25: red, X = 50: blue, X = 75: purple, X = 100: green), and (C) amorphous polymers 1 (red) and 2 (blue), measured at 77 K. The filled circles represent adsorption; the open circles represent desorption.

**Table S4.** Pore size and pore volume of the COFs.

COFsCOF	BET Surface Area (m <sup>2</sup> /g)	Pore Size (nm)	Pore Volume (cm <sup>3</sup> /g)
H <sub>2</sub> P-COF	1126	2.2	0.68
[HC≡C] <sub>25</sub> -H <sub>2</sub> P-COF	1092	2	0.66
[HC≡C] <sub>50</sub> -H <sub>2</sub> P-COF	859	1.9	0.52
[HC≡C] <sub>75</sub> -H <sub>2</sub> P-COF	324	1.5	0.16
[HC≡C] <sub>100</sub> -H <sub>2</sub> P-COF	206	1.5	0.14
[Pyr] <sub>25</sub> -H <sub>2</sub> P-COFs	960	1.9	0.56
[Pyr] <sub>50</sub> -H <sub>2</sub> P-COFs	675	1.6	0.42
[Pyr] <sub>75</sub> -H <sub>2</sub> P-COFs	86	1.4	0.025
[Pyr] <sub>100</sub> -H <sub>2</sub> P-COFs	63	1.4	0.018
Amorphous polymer 1	2	-	-
Amorphous polymer 2	0	-	-

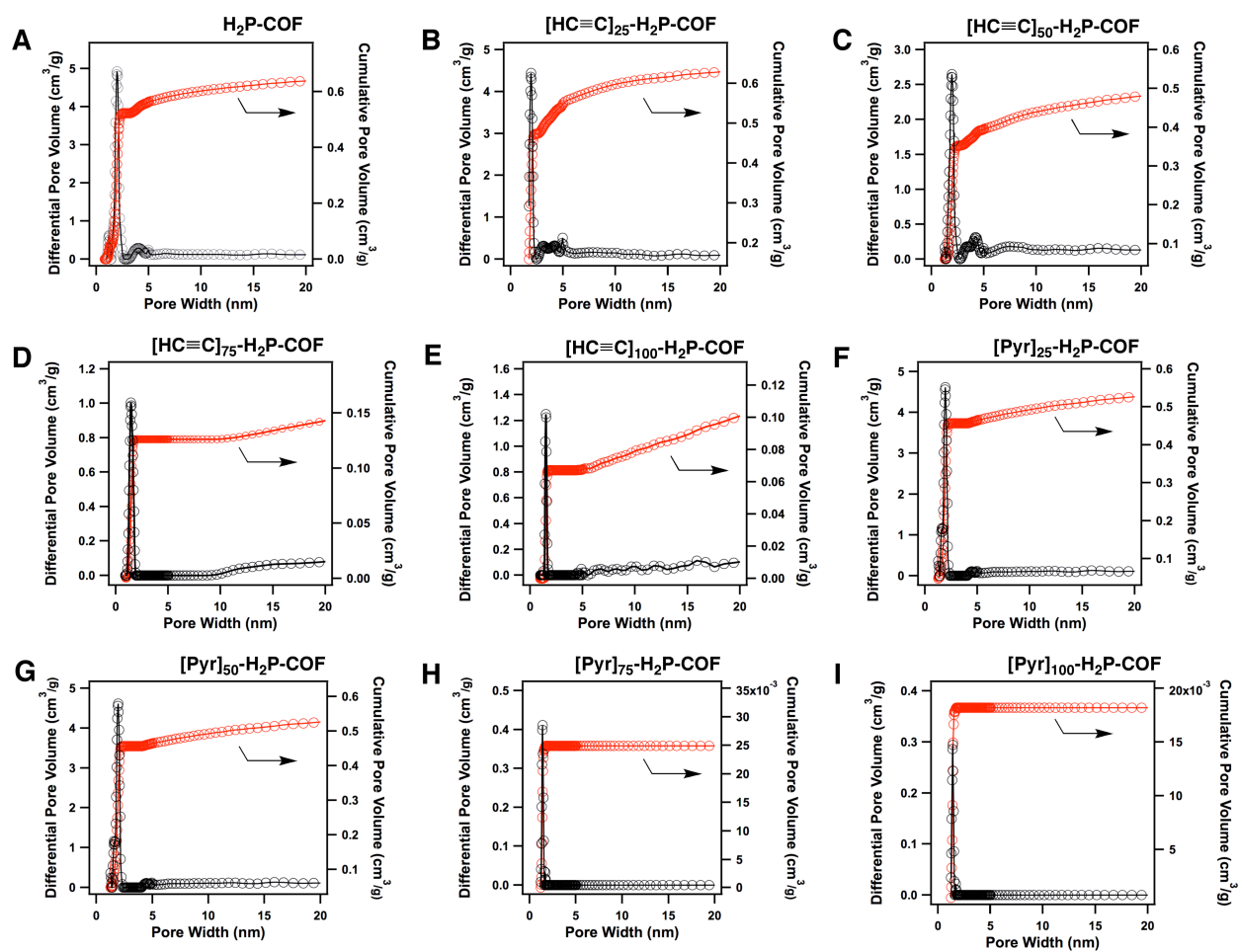
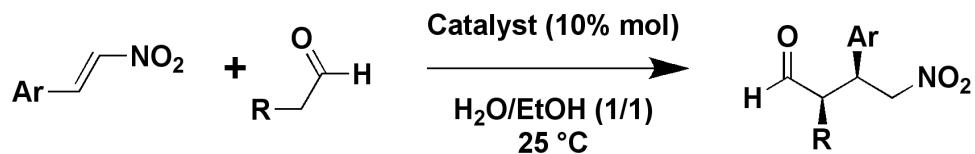


**Fig. S3.** (A-I) Pore size distribution (black) and cumulative pore volume (red) profiles of the COFs.

## H. Michael addition reactions

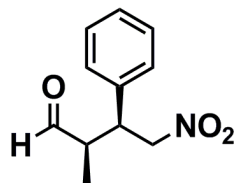
**Table S5.** Investigating the substrate scope of Michael Addition catalyzed by [Pyr]<sub>25</sub>-H<sub>2</sub>P-COF.



Product	Reaction time to 100% conversion (h)	Yield (%)	dr	ee (%)
	0.75	93	60/40	56
	0.75	94	60/40	46
	1	93	70/30	49
	1.2	94	60/40	57
	1	89	65/35	47
	1.5	88	60/40	46
	3.5	90	75/25	45

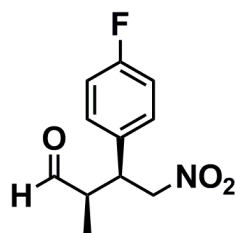
### Characterization of products

#### (2R,3S)-2-Methyl-4-nitro-3-phenylbutanal<sup>S8</sup>



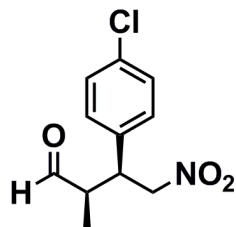
Major diastereomer: <sup>1</sup>H NMR (400 MHz, CDCl<sub>3</sub>):  $\delta$  = 9.71 (d,  $J$  = 2 Hz, 1H), 7.35-7.28 (m, 3H), 7.20-7.16 (m, 2H), 4.82-4.64 (m, 2H), 3.85-3.77 (m, 1H), 2.82-2.74 (m, 1H), 0.99 (d,  $J$  = 7.2 Hz, 3H). HPLC conditions: The enantiomeric excess was determined by HPLC (Chiralcel OD-H), hexane : *i*-PrOH = 90 : 10, UV = 214 nm, 1.0 mL min<sup>-1</sup>, syn:  $t_R$  = 22.4 min (major) and  $t_R$  = 17.6 min (minor).

#### (2R,3S)-3-(4-Fluorophenyl)-2-methyl-4-nitrobutanal<sup>S9</sup>



Major diastereomer: <sup>1</sup>H NMR (400 MHz, CDCl<sub>3</sub>):  $\delta$  = 9.70 (d,  $J$  = 1.6 Hz, 1H), 7.20-7.12 (m, 2H), 7.05-7.00 (m, 2H), 4.80-4.60 (m, 2H), 3.83-3.76 (m, 1H), 2.81-2.72 (m, 1H), 1.00 (d,  $J$  = 7.2 Hz, 3H). HPLC conditions: The enantiomeric excess was determined by HPLC (Chiralcel AD-H), hexane : *i*-PrOH = 98 : 2, UV = 214 nm, 1.0 mL min<sup>-1</sup>, syn:  $t_R$  = 33.9 min (major) and  $t_R$  = 47.0 min (minor).

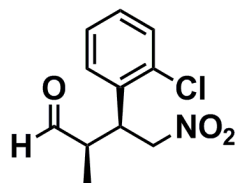
#### (2R, 3S)-3-(4-Chlorophenyl)-2-methyl-4-nitrobutanal<sup>S10</sup>



Major diastereomer: <sup>1</sup>H NMR (400 MHz, CDCl<sub>3</sub>):  $\delta$  = 9.68 (d,  $J$  = 1.2 Hz, 1H), 7.33-7.29 (m, 2H), 7.16-7.09 (m, 2H), 4.80-4.60 (m, 2H), 3.81-3.75 (m, 1H), 2.81-2.72 (m, 1H), 1.00 (d,  $J$  = 7.2 Hz, 3H). HPLC conditions: The enantiomeric excess was determined by HPLC (Chiralcel

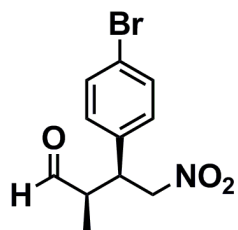
AD-H), hexane : *i*-PrOH = 98 : 2, UV = 214 nm, 1.0 ml min<sup>-1</sup>, syn:  $t_R = 41.1$  min (major) and  $t_R = 60.5$  min (minor).

(2R,3S)-3-(2-Chlorophenyl)-2-methyl-4-nitrobutanal<sup>S11</sup>



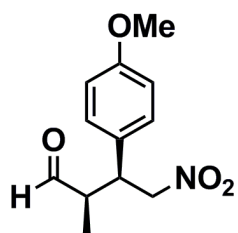
Major diastereomer: <sup>1</sup>H NMR (400 MHz, CDCl<sub>3</sub>):  $\delta = 9.73$  (d,  $J = 1.6$  Hz, 1H), 7.42-7.39 (m, 1H), 7.26-7.18 (m, 3H), 4.86-4.74 (m, 2H), 4.35-4.28 (m, 1H), 3.04-2.93 (m, 1H), 1.02 (d,  $J = 7.2$  Hz, 3H). HPLC conditions: The enantiomeric excess was determined by HPLC (Chiralcel AD-H), hexane : *i*-PrOH = 98 : 2, UV = 214 nm, 1.0 mL min<sup>-1</sup>, syn:  $t_R = 20.83$  min (major) and  $t_R = 38.0$  min (minor).

(2R,3S)-3-(4-Bromophenyl)-2-methyl-4-nitrobutanal<sup>S12</sup>



Major diastereomer: <sup>1</sup>H NMR (400 MHz, CDCl<sub>3</sub>):  $\delta = 9.68$  (d,  $J = 1.2$  Hz, 1H), 7.48-7.45 (m, 2H), 7.10-7.04 (m, 2H), 4.80-4.60 (m, 2H), 3.82-3.74 (m, 1H), 2.81-2.70 (m, 1H), 0.99 (d,  $J = 7.2$  Hz, 3H). HPLC conditions: The enantiomeric excess was determined by HPLC (Chiralcel AD-H), hexane : *i*-PrOH = 98 : 2, UV = 214 nm, 1.0 ml min<sup>-1</sup>, syn:  $t_R = 24.16$  min (major) and  $t_R = 33.93$  min (minor).

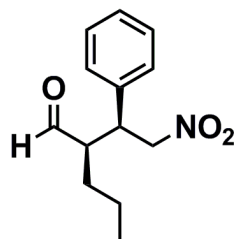
(2R,3S)-3-(4-Methoxyphenyl)-2-methyl-4-nitrobutanal<sup>S10</sup>



Major diastereomer: <sup>1</sup>H NMR (400 MHz, CDCl<sub>3</sub>):  $\delta = 9.69$  (d,  $J = 1.2$  Hz, 1H), 7.12-7.04 (m,

2H), 6.86-6.83 (m, 2H), 4.77-4.59 (m, 2H), 3.77 (s, 3H), 3.78-3.69 (m, 1H), 2.78-2.68 (m, 1H), 0.99 (d,  $J = 7.6$  Hz, 3H). HPLC conditions: The enantiomeric excess was determined by HPLC (Chiralcel OD-H), hexane : *i*-PrOH = 80 : 20, UV = 214 nm, 1.0 mL min<sup>-1</sup>, syn:  $t_R = 23.17$  min (major) and  $t_R = 20.77$  min (minor).

(R)-2-((S)-2-Nitro-1-phenylethyl)pentanal<sup>S11</sup>



Major diastereomer: <sup>1</sup>H NMR (400 MHz, CDCl<sub>3</sub>):  $\delta = 9.69$  (d,  $J = 3.6$  Hz, 1H), 7.34-7.28 (m, 3H), 7.17-7.15 (m, 2H), 4.70-4.60 (m, 2H), 3.79-3.73 (m, 1H), 2.72-2.66 (m, 1H), 1.48-1.13 (m, 4H), 0.79 (t,  $J = 7.2$  Hz, 3H). HPLC conditions: The enantiomeric excess was determined by HPLC (Chiralcel OD-H), hexane : *i*-PrOH = 90 : 10, UV = 214 nm, 1.0 mL min<sup>-1</sup>, syn:  $t_R = 23.29$  min (major) and  $t_R = 20.45$  min (minor).

## I. Recycling results

**Table S6.** Recycling experiment of the [Pyr]<sub>25</sub>-H<sub>2</sub>P-COF for the Michael addition reaction.

Catalyst	Reaction time to 100% conversion (h)	Yield (%)	dr	ee (%)	Weight
Fresh	1	93	70/30	49	>99%
Cycle 1	1.5	90	70/30	49	>99%
Cycle 2	2.6	92	70/30	48	>99%
Cycle 3	3.8	88	70/30	48	>99%
Cycle 4	4.6	86	70/30	48	>99%

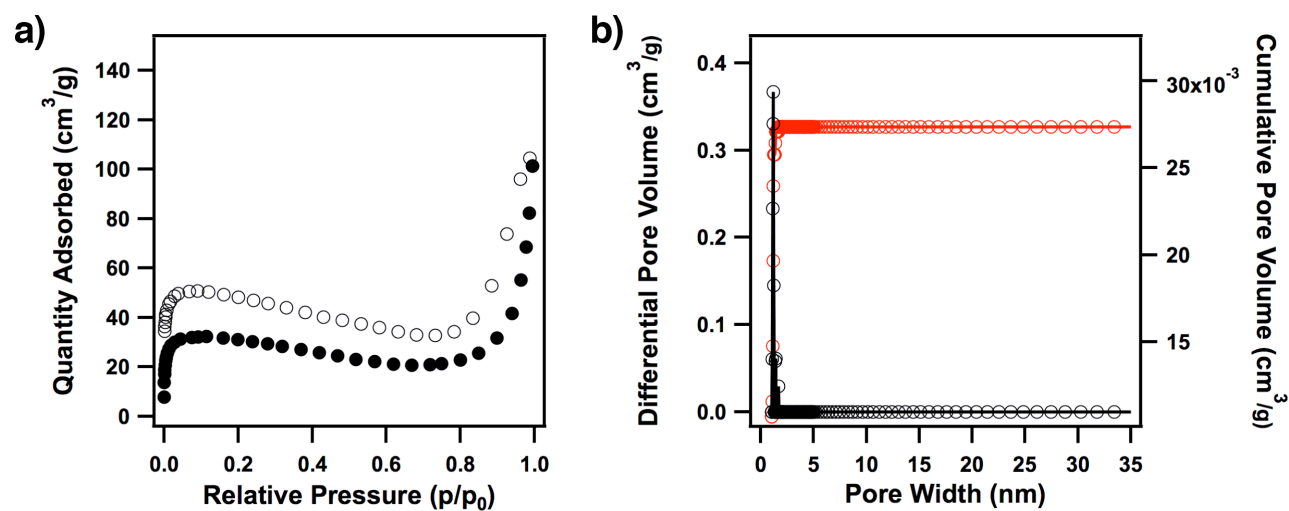


**Fig. S4.** (a) Nitrogen sorption isotherm curves of the recycled [Pyr]<sub>25</sub>-H<sub>2</sub>P-COF. (b) Pore size distribution of the recycled [Pyr]<sub>25</sub>-H<sub>2</sub>P-COF. The BET surface area is 104 m<sup>2</sup>/g.

## J. Supporting references

- S1. B. Aradi, B. Hourahine and T. Frauenheim, *J. Phys. Chem. A*, 2007, **111**, 5678-5684.
- S2. <http://www.dftb.org>.
- S3. Z. E. Brain and M. A. Addicoat, *J. Chem. Phys.*, 2011, **135**, 174106.
- S4. M. Yuasa, K. Oyaizu, A. Yamaguchi and M. Kuwakado, *J. Am. Chem. Soc.*, 2004, **126**, 11128-11129.
- S5. A. Palmgren, A. Thorarensen and J.-E. Bäckvall, *J. Org. Chem.*, 1998, **63**, 3764-3768.
- S6. V. S. P. R. Lingam, R. Vinodkumar, K. Mukkanti, A. Thomas and B. Gopalan, *Tetrahedron Lett.*, 2008, **49**, 4260-4264.
- S7. S. Luo, H. Xu, X. Mi, J. Li, X. Zheng and J. P. Cheng, *J. Org. Chem.*, 2006, **71**, 9244-9247.
- S8. J. M. Betancort and C. F. Barbas, *Org. Lett.*, 2001, **3**, 3737-3740.
- S9. R. Husmann, M. Jorres, G. Raabe and C. Bolm, *Chem.–Eur. J.*, 2010, **16**, 12549-12552.
- S10. L. Zhao, J. Shen, D. Liu, Y. Liu and W. Zhang, *Org. Biomol. Chem.*, 2012, **10**, 2840-2846.
- S11. C. A. Wang, Z. K. Zhang, T. Yue, Y. L. Sun, L. Wang, W. D. Wang, Y. Zhang, C. Liu and W. Wang, *Chem.–Eur. J.*, 2012, **18**, 6718-6723.
- S12. Y. Hayashi, H. Gotoh, T. Hayashi and M. Shoji, *Angew. Chem. Int. Ed.*, 2005, **44**, 4212-4215.